Effect of Charged Segment Length on Physicochemical Properties of Core−Shell Type Polyion Complex Micelles from Block Ionomers

Atsushi Harada† and Kazunori Kataoka*

Department of Materials Science & Engineering, Graduate School of Engineering, The University of Tokyo, 7-3-1 Hongo, Bunkyo-ku, Tokyo 113-8656, Japan

Received October 14, 2002; Revised Manuscript Received May 5, 2003

ABSTRACT: The influence of the charged segment length on the physicochemical properties of polyion complex (PIC) micelles formed from the mixture of poly(ethylene glycol)-*b*-poly(α,*β*-aspartic acid) [PEG−P(Asp)] with poly(ethylene glycol)-*b*-poly(L-lysine) [PEG−P(Lys)] or poly(L-lysine) [P(Lys)] was evaluated in this study. The hydrodynamic radius (R_h) and apparent weight-averaged molecular weight ($M_{w,app}$) of the PIC micelles were determined from the dynamic and static light scattering to calculate the association number, core radius (R_{core}), micellar radius (R_m), corona thickness (R_{corona}), and PEG density at the core/corona interface (Φ_{PEG}). Changes in R_{core} and Φ_{PEG} of the PIC micelles with a change in the charged segment length of the block copolymer were explained by considering the balance between the interfacial energy and conformational entropy of polymer strands associated in the core−shell type PIC micelles. Balance among these two parameters (R_{core} and Φ_{PEG}) seems to play a substantial role in determining micellar size, the association number, and, thus, $M_{w,app}$ of the micelles. Furthermore, Φ_{PEG} was shown to depend only on the length of the P(Asp) segment in PEG−P(Asp), regardless of the composition of the counter polycations (PEG−P(Lys) and P(Lys)). This result suggests that Φ_{PEG} might be the most crucial parameter to determine the physicochemical characteristics of the PIC micelles.

Introduction

The self-assembly of block copolymers, in particular, their micellization in selective solvents, has recently received considerable attention in various fields of polymer science. The micellization is characterized by a narrowly distributed mesoscopic size with a distinct core−shell architecture, and has been subjected to extensive studies elucidating the physicochemical features including size, association number and critical association concentration.[1−13]

The driving force of the block copolymer micellization in selective solvents is the strict difference in the solubility of each segment of the block copolymer. Thus, in aqueous medium, amphiphilic block copolymers are generally assembled into micelles with a core−shell architecture. Recently, an electrostatic interaction was found to work as the driving force of the block copolymer micellization to obtain polyion complex (PIC) micelles or block ionomer complexes, which are formed, for example, from a pair of oppositely charged block copolymers.[14,15] PIC micelles as a novel self-assembly system of block copolymers exhibit several unique features, one of which is the strict chain length recognition observed in the process of the micellization from a pair of poly(ethylene glycol)-*b*-poly(α,*β*-aspartic acid) [PEG−P(Asp)] as the aniomer and poly(ethylene glycol)-*b*-poly(L-lysine) [PEG−P(Lys)] as the catiomer.[16] The addition of PEG−P(Asp) or PEG−P(Lys) to the mixed solution of oppositely charged partners, PEG−P(Lys) for PEG−P(Asp) and PEG−P(Asp) for PEG−P(Lys), having varying chain lengths of charged segments led to the formation of PIC micelles only from a pair with a matched chain length of oppositely charged segments. The block copolymer having an unmatched chain length of the charged segment was totally segregated from the micellization. A strict phase separation between the core and corona domains of the micelles should be a critical determining factor for this chain length recognition so as to allow the formation of multimolecular micelles only from the matched pair of block copolymers satisfying both the charge stoichiometry (neutralization) in the core and the alignment of the molecular junction between the PEG and charged segment of each block copolymer strand at a core/corona interface. Note that unmatched pairs are unable to achieve a uniform distribution of ion pairs in the PIC core without the phase mixing of the PEG corona and PIC core domains.

The narrowly distributed PIC micelles were found to form even when one of the block copolymer pair with an opposite charge was changed to the corresponding simple polyelectrolyte, i.e., P(Asp) or P(Lys).[17] However, no chain length recognition occurred in this case, indicating the crucial importance of junction alignment of the block copolymer at the core/corona interface. Apparently, compared with the corresponding block copolymers (PEG−P(Asp) and PEG−P(Lys)), P(Asp) and P(Lys) have a higher freedom in their chain arrangement in the core of the PIC micelle and are not required to align their chain end to a core/corona interface. This difference in the chain alignment between the block ionomer/block ionomer and block ionomer/simple polyelectrolyte systems is certainly expected to provide distinctive physicochemical properties of the PIC micelles, including core radius, corona thickness, and PEG density at a core/corona interface, motivating us to the present study reported here to clarify the effect of the primary structure of constituent polymer strands on the PIC micellization from block ionomers.

* To whom correspondence should be addressed. Telephone: +81-3-5841-7138. Fax: +81-3-5841-7139. E-mail: kataoka@bmw.t.u-tokyo.ac.jp.

† Present address: Department of Applied Materials Science, Graduate School of Engineering, Osaka Prefecture University, 1-1 Gakuen-cho, Sakai, Osaka 599-8531, Japan.

10.1021/ma025737i CCC: $25.00
Published on Web 05/31/2003

Table 1. Number-Averaged Molecular Weight (M_n) and Molecular Weight Distribution (M_w/M_n) of Polymers Used in This Study and Increments of Refractive Index (dn/dc) of Various Solutions

samples		M_n	M_w/M_n	dn/dc exptl value	dn/dc calcd value[a]
PEG[b]		5000	1.04	0.1375	
P(Asp)[c]		6900	1.08	0.1553	
P(Lys)	C20	4100	1.12	0.1648	
	C45	9300	1.14	0.1642	
	C82	17 000	1.15	0.1647	
PEG−P(Asp)	5A18	7500	1.07	0.1428	0.1434[d]
	5A37	10 100	1.09	0.1463	0.1465[d]
	5A78	15 700	1.07	0.1491	0.1496[d]
PEG−P(Lys)	5C18	8700	1.09	0.1489	0.1486[e]
	5C35	12 300	1.10	0.1538	0.1533[e]
	5C78	21 200	1.10	0.1572	0.1579[e]
PIC micelle	5A18/5C18			0.1460	0.1464
	5A18/C20			0.1510	0.1505
	5A18/C45			0.1498	0.1503
	5A18/C82			0.1501	0.1505
	5A37/5C35			0.1508	0.1503
	5A37/C20			0.1537	0.1544
	5A37/C45			0.1546	0.1541
	5A37/C82			0.1543	0.1543
	5A78/5C78			0.1548	0.1544
	5A78/C20			0.1576	0.1573
	5A78/C45			0.1575	0.1570
	5A78/C82			0.1567	0.1573

[a] These values were calculated by using eq 6. [b] This PEG is used as initiator in block copolymer synthesis. [c] The P(Asp) used here had 50 of polymerization degree. [d] These values were calculated by using the dn/dc of PEG and P(Asp) (DP = 50). [e] These values were calculated by using the dn/dc of PEG and P(Lys) (C45).

Experimental Section

Materials. Poly(ethylene glycol)−poly(α,β-aspartic acid) block copolymers [PEG−P(Asp); PEG M_w = 5000 g/mol] having different polymerization degree (PD) of the P(Asp) segments (18, 37, and 78; the code names are 5A18, 5A37, and 5A78, respectively), poly(ethylene glycol)−poly(L-lysine) block copolymers [PEG−P(Lys); PEG M_w = 5000 g/mol] having different PD of the P(Lys) segments (18, 35, and 78; the code names are 5C18, 5C35, and 5C78, respectively), and poly(L-lysine) [P(Lys)] having different PD (20, 45, and 82; the code names are C20, C45, and C82, respectively) were synthesized as described before.[14,17−19] The number-averaged molecular weight (M_n) and molecular weight distribution (M_w/M_n) of these polymers are summarized in Table 1.

Preparation of Polyion Complex Micelles. PEG−P(Asp), PEG−P(Lys), and P(Lys) were separately dissolved in 10 mM sodium phosphate buffer (pH 7.4; $Na_2HPO_4 \cdot 12H_2O$ 2.865 g/L, $NaH_2PO_4 \cdot 2H_2O$ 0.312 g/L). PEG−P(Asp) solution was then added to the PEG−P(Lys) or P(Lys) solution in an electrically neutralized condition, i.e., [Asp]:[Lys] = 1:1, and stored overnight before the light scattering measurement.

Dynamic and Static Light Scattering. The dynamic and static light scattering measurements were carried out using DLS-700 and DLS-7000 instruments (Otsuka Electronics Co., Ltd., Osaka, Japan). Vertically polarized light of 488 nm wavelength from an Ar ion laser (15 mW and 75 mW) was used as the incident beam. All measurements were carried out at 25.0 ± 0.2 °C.

In the dynamic light scattering measurements, the autocorrelation function, g(τ), was analyzed using the cumulant method[20] in which

$$g(\tau) = \exp[-\bar{\Gamma}\tau + (\mu_2/2)\tau^2 - (\mu_3/3!)\tau^3 + ...] \quad (1)$$

yielding an average characteristic line width, $\bar{\Gamma}$. The z-averaged diffusion coefficient was obtained from the $\bar{\Gamma}$ based on the following equations:

$$\bar{\Gamma} = Dq^2 \quad (2)$$

$$q = (4\pi n/\lambda)\sin(\theta/2) \quad (3)$$

where q is the magnitude of the scattering vector, n is the refractive index of solvent, and θ is the detection angle. The measurements were performed at five angles from 30 to 150° in increments of 30° for the evaluation of the angular dependence of D, whereas the detection angle was fixed to 90° in the other measurements. The hydrodynamic radius, R_h, can then be calculated using the Stokes−Einstein equation

$$R_h = k_B T/(6\pi\eta D) \quad (4)$$

where k_B is the Boltzmann constant, T is the absolute temperature, and η is the viscosity of solvent. Also, the polydispersity index (PI = $\mu_2/\bar{\Gamma}^2$) was derived from eq 1.

In the static light scattering measurements, the light scattered by a dilute polymer solution may be expressed by the following equation

$$KC/\Delta R(\theta) = (1/M_{w,app})(1 + q^2 R_g^2/3) + 2A_2 C \quad (5)$$

where C is the concentration of the polymer, $\Delta R(\theta)$ is the difference between the Rayleigh ratio of the solution and that of the solvent, $M_{w,app}$ is the apparent weight-average molecular weight, R_g^2 is the mean square radius of gyration, A_2 is the second virial coefficient, and $K = [4\pi^2 n^2 (dn/dc)^2]/(N_A\lambda^4)$ (N_A is Avogadro's number). The known Rayleigh ratio of benzene was used as a calibration standard. The Zimm plots were made from the dependence of $\Delta R(\theta)$ on detection angle (12 angles from 40 to 150° in increments of 10°) and concentration (1.0, 2.0, 3.0, and 4.0 mg/mL). The increments of refractive index, dn/dc, of the solutions were measured using a DRM-1020 double-beam differential refractometer (Otsuka Electronics Co., Ltd., Osaka, Japan). The dn/dc of the system including several components like block copolymer micelles is expressed as a summation of dn/dc of each component:[21]

$$dn/dc = W_A(dn/dc)_A + W_B(dn/dc)_B + W_C(dn/dc)_C + ... \quad (6)$$

where $(dn/dc)_A$, $(dn/dc)_B$, and $(dn/dc)_C$ are the dn/dc values and W_A, W_B, and W_C are the weight fractions of A, B, and C components, respectively. The dn/dc values for PEG, P(Asp), P(Lys), PEG−P(Asp), PEG−P(Lys), and PIC micelles were measured, respectively. The experimentally obtained values as well as the calculated values based on eq 6 are summarized in Table 1. The experimental dn/dc values were confirmed to be in good agreement with the calculated values, which is a reasonable basis to use the experimental values summarized in Table 1 for the analysis of SLS results.

Gel Filtration Chromatography. Gel filtration chromatography (GFC) measurements were carried out in 10 mM sodium phosphate buffer with 50 mM NaCl (pH 7.4) using a column combination of Superdex 75 HR (Amersham Pharmacia Biotech, Sweden) and TSK gel G3000PW_{XL} (Tosoh Co., Tokyo, Japan). The flow rate was 0.3 mL/min, and the detection was done by refractive index at room temperature.

Results and Discussion

Hydrodynamic Radius of PIC Micelles Formed at Various Combinations. To evaluate the hydrodynamic radius of the PIC micelles prepared from various combinations of PEG−P(Asp) and PEG−P(Lys) or P(Lys), the dynamic light-scattering (DLS) measurements were carried out. All combinations of PEG−P(Asp) and P(Lys) with varying lengths gave sufficient scattering intensity to carry out the DLS measurements. However, for the PEG−P(Asp)/PEG−P(Lys) system, only a matched length pair gave an appreciable scattering intensity. Signifi-

Table 2. Hydrodynamic Radius (R_h) and Polydispersity Index (PI) of PIC Micelles[a]

anionic polymer	cationic polymer	R_h[b] (nm)	PI[c]
PEG−P(Asp)	PEG−P(Lys)		
5A18	5C18	15.8[d]	0.048
5A18	5C35		
5A18	5C78		
5A37	5C18		
5A37	5C35	16.1	0.029
5A37	5C78		
5A78	5C18		
5A78	5C35		
5A78	5C78	20.6	0.014
PEG−P(Asp)	P(Lys)		
5A18	C20	24.3[e]	0.039
5A18	C45	24.8[e]	0.047
5A18	C82	24.6	0.041
5A37	C20	24.4	0.021
5A37	C45	24.7	0.016
5A37	C82	24.5	0.032
5A78	C20	24.2[e]	0.012
5A78	C45	24.5[e]	0.029
5A78	C82	24.3	0.022

[a] The combinations of PEG−P(Asp) and PEG−P(Lys) with unmatched length of charged segments did not give enough scattering intensities to measure DLS. [b] These values were determined from the diffusion coefficient at infinite dilution using the Stokes−Einstein equation (eq 4). [c] At 2.0 mg/mL. [d] In ref 14. [e] In ref 17.

cantly lower scattering intensities were observed for the combination of unmatched pairs compared with those for the matched combinations, indicating no formation of PIC micelles with a sufficiently high association number. As will be discussed later, these unmatched pairs form the associates with a minimal association number of PEG−P(Lys) and PEG−P(Asp) for charge compensation. All measurable combinations showed no angular dependence in the diffusion coefficient (D), which is consistent with the assumed spherical shape.[21] Note that the spherical micelle formation was confirmed from the AFM observation on mica.[22] Further, the D values of the PIC micelles were independent of the concentration, suggesting the absence of secondary aggregates in the measured concentration region. Extrapolating the plots of the D value vs the concentration to zero gave the D values at infinite dilution as the y-intercept, and eventually, the hydrodynamic radii (R_h) were calculated using the Stokes−Einstein equation (eq 4 in Experimental Section). The R_h values as well as the polydispersity indices (PI) at 2.0 mg/mL obtained from the cumulant analysis are summarized in Table 2. All combinations showed low PI values (less than 0.05), indicating the formation of PIC micelles having an extremely narrow size distribution. Obviously, the change in the R_h values with the length of the charged segments followed a different trend between PEG−P(Asp)/PEG−P(Lys) and PEG−P(Asp)/P(Lys). In the former case, the R_h values increased from 16 to 21 nm with an increase in the length of the charged segments. On the other hand, the R_h values remained constant (24−25 nm) for the latter regardless of the length of the charged segments.

Influence of the Concentration on the Molecular Weight of PIC Micelles. It was reported that the PIC micelles showed a critical association behavior,[23,24] which is similar to that for block copolymer micelles formed through the differential solubility of the constituent segments in selective solvents. The influence of the critical association concentration (cac) should be taken into account for the detailed evaluation of the physicochemical properties of the PIC micelles based on static light scattering (SLS). The cac was evaluated from the Debye plots of SLS, since the scattering intensity is a sensitive function to the weight-averaged molecular weight of the solute.[25] The Debye plots of SLS, which is converted from eq 5 by the extrapolation of the detection angle (θ) to zero, is expressed as the following equation:

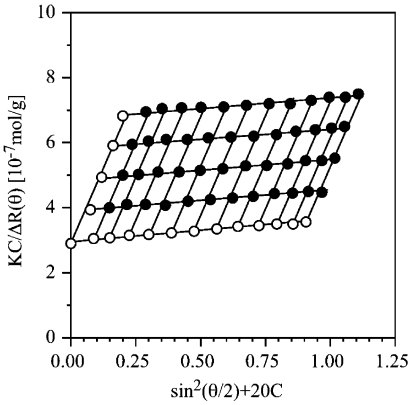

Figure 1. Zimm plots for PEG−P(Asp) (5A18)/P(Lys) (C20) (temperature, 25.0 ± 0.2 °C; detection angle, 40, 50, 60, 70, 80, 90, 100, 110, 120, 130, 140, and 150°; concentration, 1.0, 2.0, 3.0, and 4.0 mg/mL).

$$KC/\Delta R(0) = 1/M_{w,app} + 2A_2C \qquad (7)$$

By monitoring the change in the $KC/\Delta R(0)$ values with the concentration, the weight-averaged molecular weight of the solute can be evaluated. In the case of the polymeric micelles showing the critical association behavior, an increase in the $KC/\Delta R(0)$ values with a decrease in the concentration, i.e., negative A_2 values, should be observed in a concentration region below the cac due to a decrease in the averaged molecular weight.[25] All combinations of the PIC micelles followed a straight line with only a slight increase in the $KC/\Delta R(0)$ values with an increase in the concentration, reflecting the A_2 value of the PIC micelles, in the measured range from 0.01 to 4.0 mg/mL (see Supporting Information). There was no sign of a change in the $KC/\Delta R(0)$ values even in the very diluted region, suggesting that PIC micelles studied here are extremely stable upon dilution, and have no critical association concentration (cac) at least in the range higher than 0.01 mg/mL.

Evaluation of $M_{w,app}$, R_g, and A_2 for PIC Micelles. As the critical association behavior of the PIC micelles for both PEG−P(Asp)/PEG−P(Lys) and PEG−P(Asp)/P(Lys) was not observed in the concentration range of 0.01−4.0 mg/mL, the $M_{w,app}$, and R_g values were directly determined from Zimm plots in the concentration range of 1.0, 2.0, 3.0, and 4.0 mg/mL. Figure 1 shows Zimm plots for PEG−P(Asp) (5A18)/P(Lys) (C20) as a typical example. All the obtained values including $M_{w,app}$, R_g values and the association number, which was calculated from the $M_{w,app}$ value, are summarized in Table 3.

Notably, the $M_{w,app}$ values of the PEG−P(Asp)/PEG−P(Lys) system were significantly different between matched pairs and unmatched pairs of the charged segments. In the case of matched pairs, the $M_{w,app}$ values clearly depend on the length of the charged segments and increased with an increase in the length of the charged segment from 500 000 to 3 270 000 g/mol. This corresponds to the association number of PEG−

Table 3. $M_{w,app}$, R_g, R_g/R_h, Association Number, and A_2 Obtained from Static Light Scattering for the PIC Micelles

anionic polymer	cationic polymer	$M_{w,app}$[a] (g/mol)	R_g[a] (nm)	R_g/R_h	association no.[b] PEG	P(Asp)	P(Lys)	A_2[a][mL·mol/g^2] exptl[a]	calcd[c]
PEG−P(Asp)	PEG−P(Lys)								
5A18	5C18	500 000	11.8	0.747	62	31	31	7.69×10^{-5}	6.62×10^{-5}
5A18	5C35	26 200	n.d.[d]		3	2	1	5.49×10^{-3}	
5A18	5C78	52 300	n.d.[d]		5	4	1	3.76×10^{-3}	
5A37	5C18	27 300	n.d.[d]		3	1	2	6.24×10^{-3}	
5A37	5C35	890 000	11.9	0.739	80	39	41	2.68×10^{-5}	2.14×10^{-5}
5A37	5C78	43 300	n.d.[d]		3	2	1	4.11×10^{-3}	
5A78	5C18	52 800	n.d.[d]		5	1	4	4.37×10^{-3}	
5A78	5C35	42 600	n.d.[d]		3	1	2	3.81×10^{-3}	
5A78	5C78	3270 000	15.7	0.762	174	87	87	4.57×10^{-6}	3.65×10^{-6}
PEG−P(Asp)	P(Lys)								
5A18	C20	3430 000	18.2	0.749	235	235	212	1.20×10^{-5}	5.17×10^{-6}
5A18	C45	3390 000	18.7	0.754	237	237	95	1.32×10^{-5}	5.74×10^{-6}
5A18	C82	3410 000	18.5	0.752	236	236	52	1.28×10^{-5}	5.49×10^{-6}
5A37	C20	4570 000	18.4	0.754	258	258	477	3.49×10^{-6}	3.01×10^{-6}
5A37	C45	4490 000	18.7	0.757	253	253	208	3.80×10^{-6}	3.27×10^{-6}
5A37	C82	4510 000	18.6	0.759	255	255	117	3.63×10^{-6}	3.20×10^{-6}
5A78	C20	7470 000	18.0	0.744	307	307	1197	1.22×10^{-6}	1.05×10^{-6}
5A78	C45	7540 000	18.6	0.759	303	303	525	1.32×10^{-6}	1.14×10^{-6}
5A78	C82	7510 000	18.2	0.749	304	304	289	1.29×10^{-6}	1.08×10^{-6}

[a] These values were obtained from the Zimm plots at 1.0, 2.0, 3.0, and 4.0 mg/mL. [b] These values were calculated from the $M_{w,app}$ values (third column) and the number-averaged molecular weight of polymers. [c] These values were calculated from the $M_{w,app}$ values (third column) and the R_g values (forth column) using eq 8. [d] These values were not determined due to low accuracy.

P(Asp) and PEG−P(Lys) from 31 to 87 as seen in Table 3. On the other hand, the unmatched pairs had extremely lower $M_{w,app}$ values compared to those for the matched pairs. It is worthwhile to mention that, in every unmatched combination of the block copolymer, a longer chain always revealed an association number of 1.0, indicating that the PEG−P(Asp)/PEG−P(Lys) system with unmatched pair always forms a complex having a minimum association number in order to compensate their charges. These minimal charge-neutralized complexes are unable to grow further into larger PIC micelles.

As previously reported,[16] we observed a strict chain length recognition in the process of PIC micelle formation from PEG−P(Asp) (5A18 and 5A78) and PEG−P(Lys) (5C18 and 5C78). Apparently, a 4-fold difference in PD (18 and 78) is enough for a block copolymer pair to exclusively select a matched partner. It is of further interest to explore the chain length recognition between a block copolymer pair with far less difference in the length of the charged segments. Here, we examined the selection of a matched partner (5A37) by 5C35 from a mixture of unmatched components (5A18, 5A37, and 5A78) with only a 2-fold difference in the PD of the charged segments. The GFC chart for the mixture of 5A18, 5A37, and 5A78 with the same Asp unit molar concentration (6.0 mmol of Asp/mL) is shown in Figure 2a. 5A18, 5A37, and 5A78 were eluted at elution volumes of 17.5, 16.3, and 15.1 mL, respectively, although there was overlapping in the peak bottoms. As shown in Figure 2b, the peak corresponding to 5A37 obviously disappeared from the GFC chart after an addition of an oppositely charged partner, 5C35, to the mixture so as to neutralize one-third of the total Asp units in the solution. Furthermore, the concominant appearance of the peak corresponding to the PIC micelle (5A37/5C35) is obvious at an elution volume of 13.4 mL in Figure 2b. It should be noted that the GFC profile shown in Figure 2b was almost identical with that for the mixture of 5A18 and 5A78 (Figure 2c), being consistent with an exclusive selection of 5A37 from the block copolymer mixture. These GFC results clearly demonstrate that the chain length recognition in the

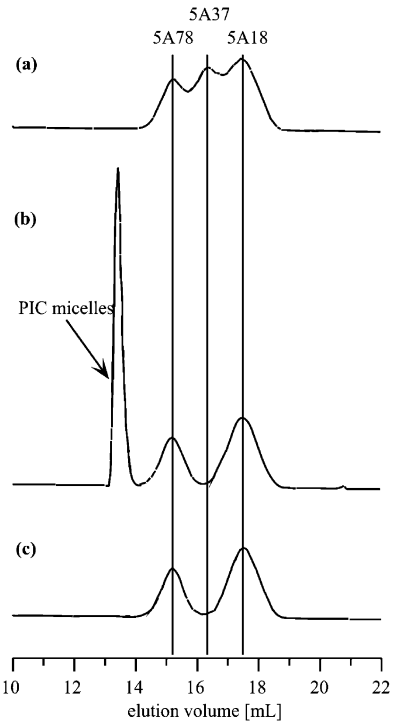

Figure 2. GFC charts for the evaluation of the chain length recognition in PIC micelle formation. (a) Mixture of three types of PEG−P(Asp) (5A18, 5A37, and 5A78) at the Asp unit concentration of 6.0 mmol of Asp /mL for each PEG−P(Asp) (total Asp unit concentration is 18.0 mmol /mL). (b) Mixture of three types of PEG−P(Asp) (same concentration as in part a) and PEG−P(Lys) (5C35: 6.0 mmol of Lys /mL). (c) Mixture of two types of PEG−P(Asp) (5A18 and 5A78) at 6.0 mmol of Asp/mL for each PEG−P(Asp).

PIC micelle formation from PEG−P(Asp) and PEG−P(Lys) is appreciably strict in nature in order to recognize the 2-fold difference in the PD of the charged segments (18, 37, and 78).

By adding a block copolymer with a definite charged segment length to the mixture of the oppositely charged block copolymers with matched and unmatched lengths of charged segments, the added block copolymer selec-

tively associated with the matched partner to form PIC micelles with an unmatched block copolymer left in the isolated form. Note that the P(Asp) segment in the PEG−P(Asp) used here is racemized with a randomly distributed sequences of α- and β-aspartic acids in the unit molar ratio of 1:3,[14] and it may not take an ordered structure including the α-helix and β-sheet, suggesting that there might be no influence of using poly(amino acid) as the charge segments on the recognition. The difference between the matched and unmatched polymer pairs may result from the prerequisite in assembly that the molecular junction between PEG and the poly(amino acid) [P(Asp) or P(Lys)] segments should align at the interface of the core and corona of each PIC micelle. On the basis of a lattice theory, unmatched pairs would encounter a long spatial restriction to align junctions for two segments of the block copolymer at this core/corona interface to maintain both the charge neutralization condition as well as a uniform segment concentration in the core. If miscibilities or phase mixing of the two segments is permitted, multimolecular association may be possible even in this case. However, this is unlikely because of the large thermodynamic penalty accompanying the phase mixing. Consequently, the association of unmatched polymer pairs remains in the minimal complex unit as indicated from the SLS data. In contrast, a matched polymer pair can readily align junctions between copolymer segments without phase mixing to form a clearly segregated core and corona comprising stoichiometric polyion complexes. Spatial alignment and assembly in PIC micelles indeed plays a crucial role in the process of the chain length recognition observed here.

The influence of the junction of the block copolymer in the formation of PIC micelles is further able to be evaluated by comparing the physicochemical properties of PEG−P(Asp)/PEG−P(Lys) and PEG−P(Asp)/P(Lys) systems, because P(Lys) need not align its chain end to the core/corona interafce. As seen in Table 3, the $M_{w,app}$ values of PEG−P(Asp)/P(Lys) were independent of the length of P(Lys) and dependent only on the length of the P(Asp) segment in PEG−P(Asp). The trend of the change in the $M_{w,app}$ values with the length of the charged segment of block copolymer was similar between PEG−P(Asp)/PEG−P(Lys) and PEG−P(Asp)/P(Lys) systems; i.e., the $M_{w,app}$ values are dependent on the length of the charged segment in the block copolymer, although the absolute $M_{w,app}$ values of the PEG−P(Asp)/PEG−P(Lys) and PEG−P(Asp)/P(Lys) systems with the same length of charged segment in the block copolymer are significantly different. The PEG−P(Asp)/P(Lys) system has a considerably larger $M_{w,app}$ value than PEG−P(Asp)/PEG−P(Lys) system. For example, the $M_{w,app}$ value of PEG−P(Asp)(5A18)/P(Lys)(C20) (3 430 000 g/mol) is seven times larger than that of PEG−P(Asp)(5A18)/PEG−P(Lys)(5C18) (500 000 g/mol). As will be discussed in the following section, this significant difference in $M_{w,app}$ reflects the difference in the association number, which is determined by the balance of several factors including the core radius, the PEG density at the core/corona interface and the conformation of PEG in the corona.

The R_g values in Table 3 followed a similar trend in terms of the chain length dependency to the R_h values summarized in Table 2. The R_g values increased with an increase in the length of the charged segment for the matched PEG−P(Asp)/PEG−P(Lys) system, whereas

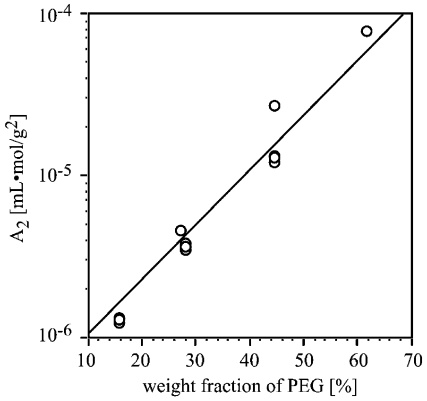

Figure 3. Relationship between the A_2 values and weight fraction of PEG segment in PIC micelles.

they remained at constant value of 18.5 nm for the PEG−P(Asp)/P(Lys) system. The ratios of the R_g to the R_h values (R_g/R_h) were then calculated, and are also summarized in Table 3. It is known that the R_g/R_h ratios for a hard sphere and a star molecule without a definite core are 0.775,[26] respectively. Assuming that the PIC micelles consist of a PIC core with a nonnegligible size and a PEG corona layer with a variance in the densities in the radial direction, it was reasonable to obtain R_g/R_h ratios of 0.739 to 0.762, which are close to a value for a hard sphere.

The Zimm plots also gave the A_2 value as summarized in Table 3. It was found that the A_2 values for the PIC micelles correlated nicely with the weight fraction of PEG as shown in Figure 3: PIC micelles with a higher PEG weight fraction exhibit a larger A_2 value. This is likely because the A_2 value mainly reflects the excluded volume effect.[12] The charged segments form the core region of the PIC micelle, which might have a small influence on an excluded volume. Consequently, the PEG corona layer has a major contribution to the excluded volume of the PIC micelle. From statistical thermodynamics, the A_2 value can be related to the radius of a hard sphere solute by the following equation:[12,28]

$$A_2 = (16\pi/3)[(N_A R_g^3)/(M_w)^2] \quad (8)$$

The A_2 values of the PIC micelles were calculated from this equation using the R_g and $M_{w,app}$ values, and are also summarized in Table 3. For all combinations, the experimental A_2 values ($A_{2,exp}$) were somewhat larger than the calculated A_2 values. Equation 8 is based on the assumption of a hard sphere having no polymer brush layer like the corona of a PIC micelle. On the other hand, the PIC micelle as the core−shell type sphere has a flexible polymer brush layer on the surface. Consequently, there might be observed a tendency to increase the A_2 value than that calculated from the R_g value.

Calculation of the Core Radius and the PEG Density at an Interface between the Core and Corona. To explore in more detail the properties of the PIC micelles, the core radius was calculated from two different physical quantities; i.e., the density of charged segments [P(Asp) and P(Lys)] and the mean volume of charged monomer units (Asp and Lys) based on the assumption that water volume in the PIC core may be negligible. In the former case, the core radius (R_{core}) can be calculated from the densities of charged segments

Table 4. Core Radius (R_{core}), PEG Density at Core−Shell Interface (Φ_{PEG}), Micellar Radius (R_m), and Corona Thickness (R_{corona})of PIC Micelles

anionic polymer	cationic polymer	R_{core} (nm) segment density[a]	R_{core} (nm) unit vol[b]	Φ_{PEG}[c] (chain/nm^2)	R_m [d] (nm)	R_{corona}[e] (nm)
PEG−P(Asp)	PEG−P(Lys)					
5A18	5C18	4.5	3.7	0.249	17.5	13.0
5A37	5C35	5.7	5.0	0.193	18.9	13.2
5A78	5C78	9.9	8.4	0.141	24.1	14.2
PEG−P(Asp)	P(Lys)					
5A18	C20	8.9	7.2	0.236	25.3	16.4
5A18	C45	8.8	7.2	0.244	25.3	16.5
5A18	C82	8.9	7.2	0.241	25.3	16.4
5A37	C20	10.6	9.4	0.183	26.4	15.8
5A37	C45	10.6	9.4	0.179	26.3	18.7
5A37	C82	10.6	9.4	0.185	26.4	15.8
5A78	C20	13.2	12.8	0.140	28.5	15.3
5A78	C45	13.2	12.8	0.138	28.5	15.3
5A78	C82	13.2	12.8	0.143	28.5	15.3

[a] These values were calculated from the density of charged segments using eq 9. [b] These values were calculated from the mean volume of charged units using eq 10. [c] These values were calculated using eq 11. [d] These values were calculated using eq 12. [e] These values were calculated using eq 13.

by the following equation:

$$R_{core} = [(^3/_4\pi)V_{core}]^{1/3} = [(^3/_4\pi)(M_{w,P(Asp)}/\rho_{P(Asp)} + M_{w,P(Lys)}/\rho_{P(Lys)})/N_A]^{1/3} \quad (9)$$

where V_{core} is the core volume of a PIC micelle, $M_{w,i}$ are the weight-averaged molecular weights of the P(Asp) and P(Lys) segments, respectively, calculated from the $M_{w,app}$ values and the weight fractions of each segment in the PIC micelles, and the ρ_i values are the densities of P(Asp) and P(Lys), respectively. The density of P(Asp) and P(Lys) were determined from pycnometric measurements to be 1.084 and 1.093 g/mL, respectively. The R_{core} values calculated from eq 9 are summarized in Table 4. On the other hand, the R_{core} values were also calculated from the mean volume of the charged monomer units from the following equation:

$$R_{core} = [(^3/_4\pi)(PD_{P(Asp)}]N_{P(Asp)}\nu_{Asp} + PD_{P(Lys)}N_{P(Lys)}\nu_{Lys})^{1/3} \quad (10)$$

where PD_i, and N_i are the polymerization degree and the association number of P(Asp) and P(Lys) in the PIC micelles, respectively. The ν_i values are the mean volume of the Asp and Lys units, and were reported to be 125 and 171 Å^3/unit, respectively.[29] The R_{core} values obtained from eq 10 are also summarized in Table 4. Obviously, the R_{core} values calculated by the two methods are in good agreement with each other. The end-to-end distances of a fully expanded model of poly(α-amino acid) segments having an 18, 36, and 78 polymerization degree are calculated to be 9.9, 19.8, and 42.1 nm, respectively.[30] The obtained R_{core} values in Table 4 suggest that the charged segments in the core of the PIC micelle might not have a fully elongated conformation. For both the PEG−P(Asp)/PEG−P(Lys) and PEG−P(Asp)/P(Lys) systems, the R_{core} values clearly increased as the polymerization degree of the P(Asp) segment in PEG−P(Asp) increased. The PEG−P(Asp)/P(Lys) system always has a larger R_{core} value than the PEG−P(Asp)/PEG−P(Lys) system when the P(Asp) length in PEG−P(Asp) is identical. For example, PEG−P(Asp)(5−18)/P(Lys)(20) (8.9 nm) has twice as large a R_{core} value as PEG−P(Asp)(5−18)/PEG−P(Lys)(5−18) (4.1 nm). This might be attributable to the difference between the degree of freedom of PEG−P(Lys) and P(Lys) in the formation of the PIC micelle with a core−shell architecture as will be discussed later.

Furthermore, the PEG density at a core/corona interface (Φ_{PEG}) was determined from the association number of the PEG segment (N_{PEG}) and the R_{core} value using the following equation:

$$\Phi_{PEG} = N_{PEG}/(4\pi R_{core}^2) \quad (11)$$

The calculated Φ_{PEG} values for various combinations are summarized in Table 4. Interestingly, all of the samples treated here, PEG−P(Asp)/PEG−P(Lys) as well as PEG−P(Asp)/P(Lys), follow the identical trend, and the Φ_{PEG} value decreased almost proportionally to an increase in the length (PD value) of the P(Asp) segment in PEG−P(Asp), although other factors such as R_h, R_g, $M_{w,app}$, and R_{core} values were significantly different among these samples. This result strongly suggests that the Φ_{PEG} value may be a crucial factor for determining the association process of the PIC micelles. The highest Φ_{PEG} value obtained here is ca. 0.25 chain/nm^2 for the system composed of PEG−P(Asp)(5A18) with the smallest occupying area of the PEG segment at an interface (4.0 nm^2/chain). The occupying area of an ethylene oxide molecule is calculated to be 0.467 nm^2/molecule using its molecular volume (0.030 nm^3).[31] Thus, the smallest occupying area of PEG at a core/corona interface of PIC micelles examined here is 8.6-times larger than the occupying area of ethylene oxide molecule itself, suggesting that the PEG segment at the core/corona interface might be sufficiently hydrated even when the PIC micelles had the highest Φ_{PEG} value. The Φ_{PEG} values decreased from 0.25 to 0.14 chain/nm^2 with an increase in the length of the P(Asp) segments as summarized in Table 4. This change might influence the conformation of the PEG segments. To evaluate the change in the PEG conformation, the micellar radius (R_m) was determined based on the model reported by Vagberg et al.,[27] and the corona thickness (R_{corona}) was calculated using the following equations:

$$R_m = \left(\frac{8\,N_s f^{(1-\upsilon)/2\upsilon}}{3(4^{1/\upsilon})\upsilon}\,a_s^{1/\upsilon} + R_{core}^{1/\upsilon}\right)^{\upsilon} \quad (12)$$

$$R_{corona} = R_m - R_{core} \quad (13)$$

N_s, f, and a_s are polymerization degree, association

number, and the size of monomers of shell-forming segment. In the model of Vagberg et al., the radial density distribution of polymer segments is expressed as $\rho(r) \propto f^{(3\nu-1)/2\nu} r^{(1-3\nu)/\nu}$, which varies with f according to the exponent $\nu = {}^1/_2$ for near Θ conditions. The calculated R_m and R_{corona} values were also summarized in Table 4. The R_m values were slightly larger than the R_h values. Such slightly increased R_m values compared to R_h values was also observed for PEG−polystyrene block copolymer (PEG−PSt) micelles by Vagverg et al. because of some draining in the outer portions of the starlike micelles. The difference between R_m and R_h for PIC micelles evaluated here might be attributed to the same reason for these PEG−PSt micelles. There were opposite trends for the change in the R_{corona} values between the PEG−P(Asp)/PEG−P(Lys) and PEG−P(Asp)/P(Lys) systems. The R_{corona} of PEG−P(Asp)/P(Lys) was slightly decreased from 16.5 to 15.3 nm with an increase in the length (PD value) of the P(Asp) segments. On the other hand, the R_{corona} of PEG−P(Asp)/PEG−P(Lys) increased from 13.0 to 14.2 nm with PD of the P(Asp) segments. However, the change in R_{corona} for both PEG−P(Asp)/P(Lys) and PEG−P(Asp)/PEG−P(Lys) were quite small (1.2 nm) and it may be safe to assume that R_{corona} retained constant value despite the change in the Φ_{PEG} values with the polymerization degree of the P(Asp) segment, suggesting that an increase in Φ_{PEG} provided a small influence to PEG conformation.

Conclusion

For core−shell type PIC micelles from both the PEG−P(Asp)/PEG−P(Lys) and PEG−P(Asp)/P(Lys) systems, the state of the block copolymer junction at an interface between the core and corona has significant importance in order to determine their physicochemical properties including the association number, hydrodynamic radius as well as core radius. The requirement for the decreasing excess free energy at the core−corona interface drives the PIC micelles to increase in association number, allowing to lower the relative surface area of the interface. This increase in the association number is accompanied by an increase in the core radius. Naturally, there exists a limitation in the increase in the core radius, because the core-forming segment, whose junction with the corona-forming segment should align at the interface, must take a more stretched conformation with the larger core radius. The increase in the association number also induces an increase in the density of the corona segments at a core/corona interface. This is also thermodynamically unfavorable, since the corona-forming segment must take a more stretched conformation. The stretching of the core- as well as corona-forming segments with an increased association number results in a decrease in the conformational entropy, which should compensate for the decreased interfacial free energy upon micellization. It is this balance between the interfacial free energy and conformational entropy of the polymer strands that determines the thermodynamically stable size of the PIC micelles with a core−shell structure. Consequently, the thermodynamical balance certainly reflects the physicochemical properties of the micelles including the core radius, corona thickness and PEG density at the core/corona interface. In particular, the PEG density at the core/corona interface might be the most crucial parameter in PIC micelle formation, because this parameter depends only on the length of the charged segment in the block copolymer and there was observed no difference between the PEG−P(Asp)/PEG−P(Lys) and PEG−P(Asp)/P(Lys) systems when the composition of PEG−P(Asp) is identical.

Acknowledgment. This work was financially supported by a Grant-in-Aid for Scientific Research from the Ministry of Education, Culture, Sports, Science, and Technology (MEXT), Japan, and by Core Research for Evolutional Science and Technology (CREST), Japan Science and Technology Corp. (JST).

Supporting Information Available: Figures showing the Debye plots of SLS for PEG−P(Asp)/PEG−P(Lys) and PEG−P(Asp)/P(Lys)(C45). This material is available free of charge via the Internet at http://pubs.acs.org.

References and Notes

(1) Tuzar, Z.; Kratochvíl, P. *Adv. Colloid Interface Sci.* **1976**, *6*, 201.
(2) Zhou, Z.; Chu, B. *J. Colloid Interface Sci.* **1988**, *126*, 171.
(3) Zhao, C.-L.; Winnik, M. A.; Riess, G.; Croucher, M. D. *Langmuir* **1990**, *6*, 514.
(4) Cao, T.; Munk, P.; Ramireddy, C.; Tuzar, Z.; Webber, S. E. *Macromolecules* **1991**, *24*, 6300.
(5) Qin, A.; Tian, M.; Ramireddy, C.; Webber, S. E.; Munk, P.; Tuzar, Z. *Macromolecules* **1994**, *27*, 120.
(6) Prochazka, K.; Martin, T. J.; Munk, P.; Webber, S. E. *Macromolecules* **1996**, *29*, 6518.
(7) Zhang, L.; Eisenberg, A. *Science* **1995**, *268*, 1728.
(8) Astafieva, I.; Khougaz, K.; Eisenberg, A. *Macromolecules* **1995**, *28*, 7127.
(9) Moffitt, M.; Khougaz, K.; Eisenberg, A. *Acc. Chem. Res.* **1996**, *29*, 95.
(10) Kwon, G.; Naito, M.; Yokoyama, M.; Okano, T.; Sakurai, Y.; Kataoka, K. *Langmuir* **1993**, *9*, 945.
(11) Cammas, S.; Kataoka, K. *Macromol. Chem. Phys.* **1995**, *196*, 1899.
(12) Nolan, S. L.; Phillips, R. J.; Cotts, P. M.; Dungan, S. R. *J. Colloid Interface Sci.* **1997**, *191*, 291.
(13) Förster, S.; Zisenis, M.; Wenz, E.; Antonietti, M. *J. Chem. Phys.* **1996**, *104*, 9956.
(14) Harada, A.; Kataoka, K. *Macromolecules* **1995**, *28*, 5294.
(15) Kabanov, A. V.; Bronich, T. K.; Kabanov, V. A.; Yu, K.; Eisenberg, A. *Macromolecules* **1996**, *29*, 6797.
(16) Harada, A.; Kataoka, K. *Science* **1999**, *283*, 65.
(17) Harada, A.; Kataoka, K. *J. Macromol. Sci.—Pure Appl. Chem.* **1997**, *A34*, 2119.
(18) Yokoyama, M.; Inoue, S.; Kataoka, K.; Yui, N.; Sakurai, Y. *Macromol. Chem. Rapid Commun.* **1987**, *8*, 431.
(19) Yokoyama, M.; Inoue, S.; Kataoka, K.; Yui, N.; Okano, T.; Sakurai, Y. *Makromol. Chem.* **1989**, *190*, 2041.
(20) Koppel, D. E. *J. Chem. Phys.* **1972**, *57*, 4814.
(21) Xu, R.; Winnik, M. A.; Hallett, F. R.; Riess, G.; Croucher, M. D. *Macromolecules* **1991**, *24*, 87.
(22) Harada, A.; Kataoka, K. *Macromol. Symp.* **2001**, *172*, 1.
(23) Kabanov, A. V.; Bronich, T. K.; Kabanov, V. A.; Yu, K.; Eisenberg, A. *Macromolecules* **1996**, *29*, 6797.
(24) Harada, A.; Kataoka, K. *Langmuir* **1999**, *15*, 4208.
(25) Khougaz, K.; Gao, Z.; Eisenberg, A. *Macromolecules* **1994**, *27*, 6341.
(26) Douglas, J. K.; Roovers, J, Freed, K. F. *Macromolecules* **1990**, *23*, 4168.
(27) Vagberg, L. J. M.; Cogan, K. A.; Gast, A. P. *Macromolecules* **1991**, *24*, 1670.
(28) Khougaz, K.; Zhong, X. F.; Eisenberg, A. *Macromolecules* **1996**, *29*, 3937.
(29) Chothia, C. *Annu. Rev. Biochem.* **1984**, *53*, 537.
(30) Pauling, L.; Corey, R. B. *Proc. Int. Wool Text. Res. Conf.* **1955**, *B*, 249.
(31) Nagarajan, R.; Ganesh, K. *J. Colloid Interface Sci.* **1996**, *184*, 489.

MA025737I